

FERMILAB-CONF-21-377-QIS-SCD-T

DIS physics at the EIC and LHeC and connections to the future LHC and νA programs

T. J. Hobbs^{1,2,3,4,*}¹ Fermi National Accelerator Laboratory, Batavia, IL 60510, USA² Department of Physics, Illinois Institute of Technology, Chicago, IL 60616, USA³ EIC Center, Jefferson Lab, Newport News, VA 23606, USA⁴ Department of Physics, Southern Methodist University, Dallas, TX 75275, USA

* thobbs@fnal.gov

August 22, 2021



*Proceedings for the XXVIII International Workshop
on Deep-Inelastic Scattering and Related Subjects,
Stony Brook University, New York, USA, 12-16 April 2021
doi:[10.21468/SciPostPhysProc.7](https://doi.org/10.21468/SciPostPhysProc.7)*

1

2 Abstract

3 Deeply-inelastic scattering (DIS) stands to enter a golden age with the prospect of pre-
4 cision programs at the Electron-Ion Collider (EIC) and Large Hadron-electron Collider
5 (LHeC). While these programs will be of considerable importance to resolving longstand-
6 ing issues in (non)perturbative QCD as well as hadronic and nuclear structure, they will
7 also have valuable implications for a wider range of physics at the Energy and Intensity
8 Frontiers, including at the High-Luminosity LHC (HL-LHC) and future νA facilities. In
9 this plenary contribution, we highlight a number of salient examples of the potential
10 HEP impact from the complementary EIC and LHeC programs drawn from their respec-
11 tive Yellow Report and Whitepaper. Interested readers are encouraged to consult the
12 extensive studies and literature from which these examples are taken for more detail.

13

14 Contents

15	1 Introduction	2
16	2 High-energy reach of the EIC	3
17	2.1 EIC brief review	3
18	2.2 Tomography implications of the EIC for HEP	4
19	3 Precision DIS for HEP at the LHeC	7
20	3.1 LHeC brief review	7
21	3.2 EW measurements and SM tests at the LHeC	7
22	4 Conclusion	8
23	References	9

24
2526 **1 Introduction**

27 The past several years have witnessed rapid development in the areas of hadronic structure
 28 and QCD as well as in efforts to test the standard model (SM) of particle physics at both the
 29 Energy and Intensity Frontiers. Rather than being isolated one from the other, deep comple-
 30 mentarities connect the progress being made on these various fronts. In particular, a crucial
 31 link among the activities in these areas is the central role of deeply-inelastic scattering (DIS)
 32 as a sensitive probe of the internal structure of hadrons and nuclei — a fact which follows
 33 mainly from the experimental ‘cleanliness’ of the DIS process, as well as its ability to furnish
 34 a kinematical lever-arm by measuring structure functions or DIS cross sections over diverse
 35 scales to constrain DGLAP scaling violations. Additionally, theoretical control over the pure
 36 DIS process has achieved a high level of theoretical accuracy, with NNLO and, increasingly,
 37 N³LO the state-of-the-art in determining Wilson coefficients and related quantities. Critically,
 38 DIS provides direct access to the parton distribution functions (PDFs) of the nucleon [and anal-
 39 ogous nuclear PDFs (nPDFs) for nuclear targets]. The PDFs are an essential nonperturbative
 40 input required for hadronic collider experiments. For instance, for the inclusive hadroproduc-
 41 tion, $pp \rightarrow W/Z + X$, of electroweak (EW) bosons, the ability to predict SM contributions to
 42 the cross section follows from knowledge of the perturbatively calculable parton-level cross
 43 section, $\hat{\sigma}$, and the PDFs of the colliding protons:

$$\sigma(AB \rightarrow W/Z + X) = \sum_n \alpha_s^n \sum_{a,b} \int dx_a dx_b f_{a/A}(x_a, \mu^2) \hat{\sigma}_{ab \rightarrow W/Z+X}^{(n)}(\hat{s}, \mu^2) f_{b/B}(x_b, \mu^2). \quad (1)$$

44 Although precision in tests of the SM is potentially limited by an array of experimental system-
 45 atic as well as theoretical uncertainties, PDF uncertainties are likely to increasingly dominate
 46 the landscape of error sources. This logic applies to Higgs-production cross sections, W -mass
 47 determinations, extractions of $\sin^2 \theta_W$, and a multitude of searches — direct and indirect —
 48 for beyond SM (BSM) physics at the LHC. Conversely, extending to lower energies, knowledge
 49 of the PDFs and related quantities are an important limitation in Intensity Frontier activities
 50 entailing searches for a potential CP-violating phase, δ_{CP} , at long-baseline neutrino facilities.
 51 Such efforts require detailed knowledge of the neutrino-nuclear interactions in the few-GeV
 52 regime, including νA DIS. Here, control over the PDFs and power-suppressed corrections of
 53 relevance at lower Q^2 and W^2 is a primary limitation in the realization of the required preci-
 54 sion. As a result, high-quality DIS information will play a valuable role in extending the general
 55 precision and sensitivity to BSM physics at both the HL-LHC [1] and future νA facilities like
 56 DUNE [2].

57 In these proceedings, we present a brief overview of two future DIS programs: the US-
 58 based Electron-Ion Collider (EIC) [3, 4] and Large Hadron-electron Collider (LHeC) [5] pro-
 59 posed for construction at CERN. In particular, we illustrate how these programs can be ex-
 60 pected to significantly impact precision activities at the LHC and future High-Luminosity LHC
 61 (HL-LHC). A valuable aspect of the future DIS programs to be carried out at the EIC and LHeC
 62 is their ability to probe complementary regions of the kinematical (x, Q^2) plane as shown in
 63 Fig. 1. In particular, the energy and expected luminosity of the EIC program, which we discuss
 64 in greater detail in Sec. 2, is such that its primary focus spans the few-GeV (non)perturbative
 65 boundary region at very high x and low Q^2 , but with robust reach down to $x \sim 10^{-4}$ and
 66 $Q^2 \sim 1000 \text{ GeV}^2$ at larger x . The ability of the EIC to unravel dynamics in the few-GeV tran-

67 sition region to perturbative QCD interactions also applies to studies involving nuclei, as il-
 68 lustrated in Fig. 1 (right). The LHeC discussed in Sec. 3, in contrast, will have the ability
 69 to probe very low $x \sim 10^{-6}$ over a significant range of Q^2 momenta, and will be capable of
 70 probing perturbative scales as high as $Q^2 \sim 10^{5-6} \text{ GeV}^2$ by merit of its TeV-regime kinematics.
 71 In consequence of this wide reach, the LHeC would be capable of interrogating overlapping
 72 kinematical regions covered by the HL-LHC, but through measurements of complementary DIS
 73 processes. We highlight specific operational parameters responsible for the unique scope of
 74 the EIC and LHeC programs in respective, dedicated subsections below.

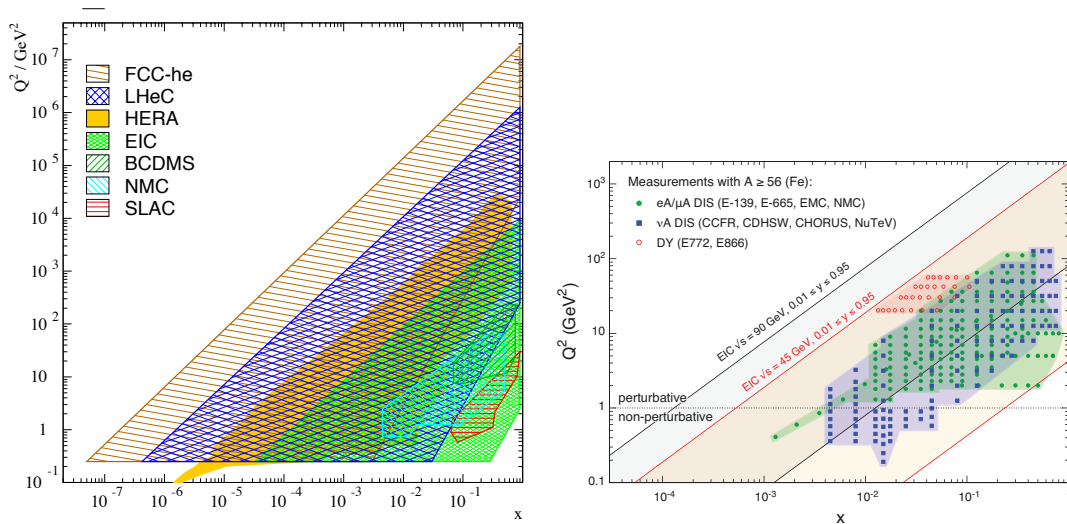


Figure 1: (Left) The kinematical coverage of various legacy and upcoming/proposed DIS experiments in x and Q^2 , from Ref. [5]. The wide kinematical coverage of both the EIC and LHeC intersect the regions probed by older fixed-target DIS experiments while extending into novel regions of low x and large Q^2 . (Right) A complementary map of the kinematical coverage of the EIC in DIS measurements involving heavier nuclei ($A \geq 56$); superposed are the placements of legacy data sets involving charged-lepton, νA , and Drell-Yan (DY) information; taken from Ref. [4].

75 We also emphasize that the issues mentioned in these brief proceedings are a small but rep-
 76 resentative sub-sample of the numerous points extensively canvassed in the main community
 77 literature of the two facilities discussed here: for the EIC, the recent Yellow Report of Ref. [3];
 78 and for the LHeC, the similarly recent whitepaper, Ref. [5]. We refer interested readers to
 79 these documents, which have dedicated sections related to many of the examples noted here.

80 2 High-energy reach of the EIC

81 2.1 EIC brief review

82 We quickly summarize some of the specifics of the upcoming EIC program [3] from which
 83 its unique capabilities for QCD and hadronic physics are derived. Having recently received
 84 CD-1 approval from the DOE for development at Brookhaven's RHIC facility, the EIC will be
 85 a next-generation DIS collider and the effective successor to the impactful HERA program at
 86 DESY, with significantly greater instantaneous luminosity (by a factor of 10^{2-3}). This enhanced
 87 luminosity is expected to produce an expansive set of DIS data, of magnitude $\int dt \mathcal{L} \sim 1 \text{ ab}^{-1}$.
 88 The EIC will collide electrons with a variety of nuclear targets, including the proton, deuteron,
 89 and ^3He ; electron-nuclear collisions involving, *e.g.*, uranium, will allow a broad program for

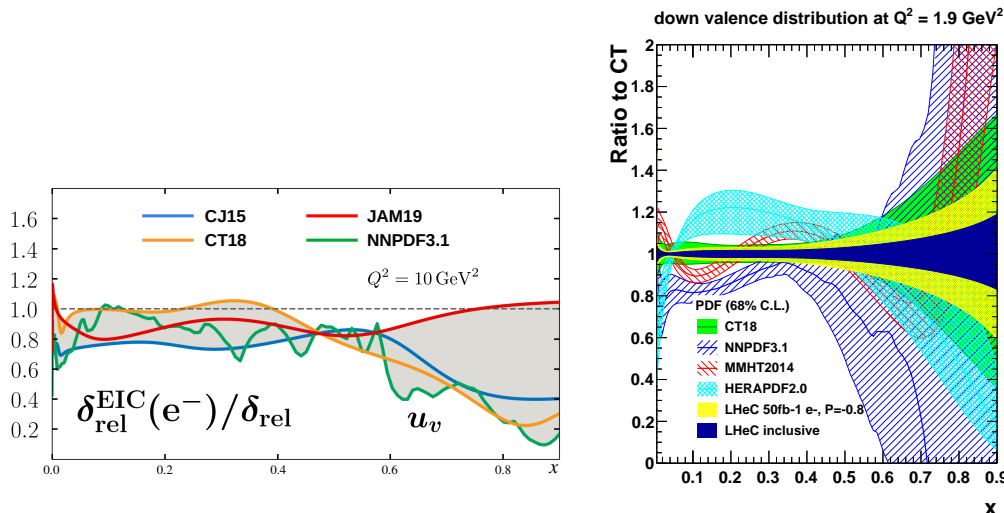


Figure 2: The EIC and LHeC will have significant constraining power of the unpolarized PDFs of the nucleon, as illustrated here for select examples. (Left) The EIC will have the potential to reduce high- x uncertainties of the u_v PDF; adapted from Ref. [3], we plot the relative uncertainty on $u_v(x)$ at $Q^2 = 10 \text{ GeV}^2$ after including 100 fb^{-1} of e^- EIC pseudodata, which can reduce PDF uncertainties by as much a factor of ~ 5 at $x \sim 0.8$. (Right) Analogously, analyses carried out using the xFitter framework [6] suggest that LHeC inclusive measurements can cut down the PDF uncertainty on the d_v PDF by several factors at high x . Such reductions in high- x valence-PDF uncertainties will be instrumental for enhancing the precision of BSM searches in, e.g., the tails of rapidity distributions in high-mass Drell-Yan at the HL-LHC. Panel taken from Ref. [5].

90 charged-lepton nuclear DIS. For ep scattering, the EIC will be capable of collisions with $E_e \leq 18$
 91 GeV and $E_p \leq 275$ GeV, offering substantial kinematical coverage in center-of-mass energy,
 92 $20 \leq \sqrt{s} \leq 140$ GeV. Although not generally included in baseline scenarios in the recent Yellow
 93 Report [3], possible facility upgrades may allow analogous studies using positron beams, which
 94 could open a number of channels for explorations of charge-symmetry violation [7] in the
 95 deuteron system as well as BSM physics. Critically, the EIC will supply electrons with up to
 96 80% beam polarization for collisions with unpolarized light and heavy nuclei. In addition,
 97 scattering with polarized proton and light-nuclear beams will also be available for thorough
 98 dissections of the spin structure of the nucleon.

99 2.2 Tomography implications of the EIC for HEP

100 The EIC is a machine chiefly targeted at understanding (non)perturbative QCD and its implica-
 101 tions for the properties of hadrons (including the light mesons [9]) and nuclei, encompassing
 102 the multi-dimensional or *tomographic* structure of these strongly-bound systems. To realize
 103 these objectives, the EIC program will consist of an extensive agglomeration of measurements
 104 of DIS cross sections and observables of varying inclusivity which will constrain PDFs, TMDs,
 105 GPDs, and hadronic and nuclear form factors — directly impacting the precision limitations
 106 of LHC and νA measurements that depend on knowledge of these quantities. The EIC will
 107 therefore be capable of sharply resolving the unpolarized PDFs of the proton, including the
 108 valence PDFs like $u_v(x, Q)$ for which we plot in Fig. 2 (left) the EIC-driven uncertainty reduc-
 109 tions recently calculated for the EIC Yellow Report, Ref. [3]; improvements will also extend to
 110 the gluon content and flavor structure of the light-quark sea of importance to Intensity Frontier
 111 work in the EW sector. In this respect, the EIC will be a valuable follow-up to fixed-target Drell-

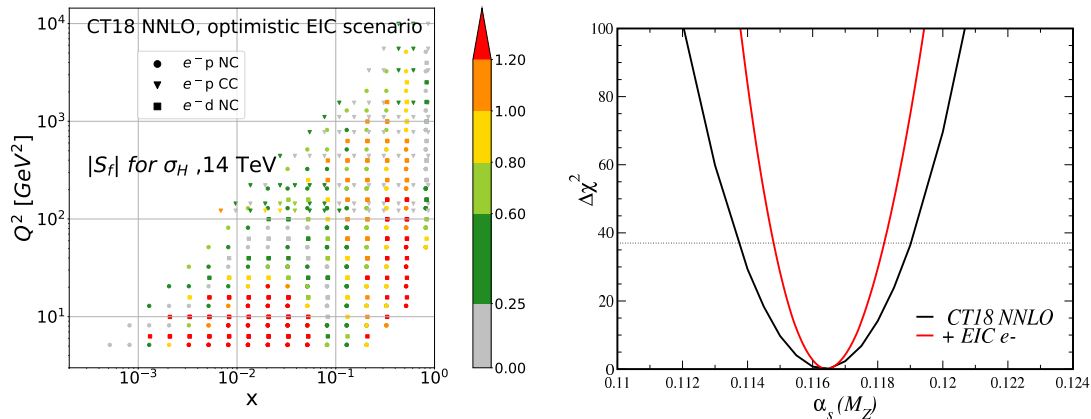


Figure 3: The PDF sensitivity of the 100 fb^{-1} EIC pseudodata explored in the EIC Yellow Report translates into a substantial point-by-point impact on the SM Higgs production cross section (left), as visualized using the PDFSense methodology [8]. Similarly, extensive DIS collisions covering a range of scales and x values results in important potential constraints on the strong coupling, α_s (right); the precision on α_s can improve by $\sim 40\%$ over the corresponding uncertainty in CT18 NNLO following the inclusion and analysis of 100 fb^{-1} of electron-scattering data. Both panels are taken from Ref. [3].

112 Yan measurements like the recent FNAL SeaQuest (E906) experiment [10]. At this meeting,
 113 we presented some preliminary PDF analysis results, discussed in greater detail in Ref. [11],
 114 of the new SeaQuest σ^{pd}/σ^{pp} data, along with other recent developments in the CT18 NNLO
 115 PDF framework [12].

116 Beyond the leading-twist unpolarized PDFs of most immediate relevance to LHC predic-
 117 tions, the EIC in particular will undertake a DIS program beyond fully-inclusive measurements.
 118 This will include a variety of transverse-momentum dependent (TMD) quantities with poten-
 119 tial sensitivity to the TMD PDFs and fragmentation functions of the proton. Such measure-
 120 ments provide an additional setting to perform further test of factorization theorems of QCD
 121 as well as measurements of TMD PDFs related to W -mass determinations [13]. In addition to
 122 tomographic measurements, the EIC will also have a dedicated program related to perturbative
 123 QCD, with the capability of imposing stringent constraints on the strong coupling, α_s , heavy-
 124 quark masses, and EW observables. This will be in conjunction with a proposed program to
 125 investigate, *e.g.*, DIS jet production, single-inclusive hadron production, and other processes
 126 which test QCD in the perturbative regime and facilitate studies of the applicability and range
 127 of validity of various QCD factorization theorems. In addition, processes like charge-current
 128 DIS jet production [14] may unlock novel channels with especially strong sensitivity to the nu-
 129 cleon’s strange content, which also has significant implications for realizing next-generation
 130 precision in the EW sector.

131 Regarding the EIC’s potential tomography-mediated impact on HEP observables, we show
 132 in the left panel of Fig. 3 the PDF sensitivity of EIC pseudodata to the SM Higgs-production
 133 cross section at LHC energies (here, $\sqrt{s} = 14 \text{ TeV}$), calculated using the PDFSense pack-
 134 age [8]. These findings were developed in the context of the CT18 NNLO PDF set in sup-
 135 port of the EIC Yellow-Report Initiative. The pseudodata appearing in Fig. 3 (left) assume
 136 100 fb^{-1} of DIS data in the form of inclusive reduced cross, $\sigma(x, y, Q^2)$, from neutral-current
 137 (NC) and charged-current (CC) e^-p scattering and NC e^-d interactions. The information here
 138 presumes an “optimistic” scenario for the systematic uncertainties. We note that the pseu-

139 dodata here are those that drove the PDF improvement plotted in Fig. 2 (left), but are now
 140 mapped point-by-point to their respective values of (x, Q^2) and scored according to their pull
 141 on $\sigma_H(\sqrt{s} = 14 \text{ TeV})$; redder points indicate those data with stronger sensitivity to the in-
 142 clusive Higgs cross section. We emphasize that the strong PDF sensitivity to σ_H appearing
 143 in Fig. 2 (left) reflects the incisive constraints the EIC will place on the proton's gluon PDF,
 144 which propagate to SM predictions for Higgs production in pp scattering through the domi-
 145 nant $gg \rightarrow H$ channel. Analogous PDF-driven improvements from the EIC can be expected
 146 to power enhancements in extractions of m_W , $\sin^2 \theta_W$, and other PDF-dependent searches for
 147 BSM physics at the HL-LHC. Measuring inclusive DIS cross sections over a wide range of scales
 148 is informative at the level of perturbative QCD in addition to parton distributions. We show
 149 this by plotting the uncertainty on $\alpha_s(M_Z)$ in the right panel of Fig. 3, which we obtain by re-
 150 fitting the default parametrization and data sets of CT18 NNLO over a series of chosen values
 151 of $\alpha_s(M_Z)$ in the presence of the EIC pseudodata described above. The resulting $\Delta\chi^2$ growth
 152 profile obtained as $\alpha_s(M_Z)$ is varied can then be compared to the corresponding series of fits
 153 without the EIC pseudodata; this reveals a $\sim 40\%$ reduction in the 1σ -uncertainty on $\alpha_s(M_Z)$.
 154 Similar exercises involving other QCD-sector SM inputs like the heavy-quark masses imply a
 155 powerful potential for exploring perturbative QCD at the EIC.

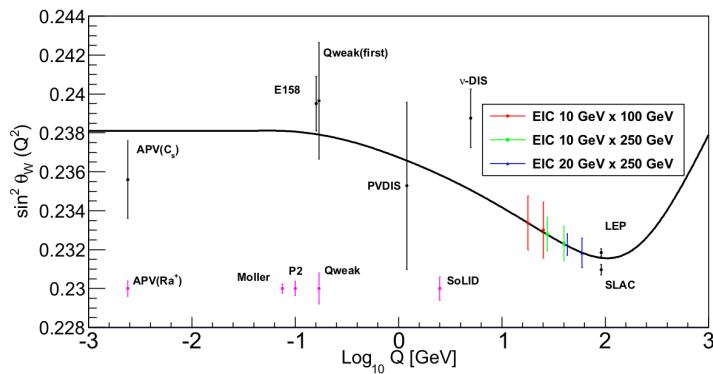


Figure 4: By measuring parity-violating DIS at the EIC, new coverage and precision can be introduced in determinations of $\sin^2 \theta_W$, as shown in this plot from Ref. [15]; this assumes an integrated luminosity of 400 fb^{-1} .

156 Finally, we point out that the EIC will have at its disposal the ability to perform a number of
 157 more direct probes for BSM physics, including leptoquark searches for charged-lepton flavor
 158 violation (CLFV), as well as precise constraints to $\sin^2 \theta_W$ through parity-violating DIS mea-
 159 surements. In the case of $\sin^2 \theta_W$ measurements, the EIC would have significant constraining
 160 power over extensions of the EW sector, including scenarios involving the presence of hypo-
 161 theoretical Z' bosons [15] as represented in Fig. 4. Also noteworthy, *polarized* electron-proton
 162 DIS at the EIC has the potential to probe specific Wilson-coefficient combinations otherwise
 163 challenging to access purely through pp scattering data in the context of SM effective field
 164 theory (SMEFT) fits as discussed in Ref. [16]. Moreover, the high-precision nuclear physics
 165 program at the EIC will similarly entail studies of nuclear-medium effects on parton distribu-
 166 tions as well as DIS jet production from nuclei and explorations of nuclear jet quenching. This
 167 work will be informative for AA scattering at the LHC, and can be expected to benefit, *e.g.*,
 168 investigations of ultra-peripheral collisions (UPCs).

169 3 Precision DIS for HEP at the LHeC

170 3.1 LHeC brief review

171 As with the EIC, we provide a quick overview of the specific parameters of the envisioned LHeC
 172 facility. Like the EIC, the LHeC is a proposed DIS machine with extremely high instantaneous
 173 luminosity, but also possesses the capability to extend DIS to the TeV scale for the first time. The
 174 LHeC would accomplish this by constructing an Energy Recovery LINAC (ERL) to provide an
 175 electron beam into the HL-LHC complex (or that of the Future Circular Collider, in the FCC-*eh*
 176 proposal). Kinematically, the LHeC could thus achieve center-of-mass energies of $\sqrt{s} = 1.2, 1.3$
 177 TeV by colliding $E_e = 50, 60$ GeV electrons with protons having the $E_p = 7$ TeV beam energy
 178 currently available at the LHC. Strong electron-beam polarizations with $P_e = \pm 0.8$ would also
 179 be possible. By extending DIS to the TeV scale, the LHeC would offer a sweeping range of
 180 channels and possible measurements to examine QCD at high energies — including probes of
 181 the gluon and quark PDFs like $d_v(x, Q)$ shown in Fig. 2 (right) to both high and very low x ,
 182 $x \geq 5 \times 10^{-5}$ — as well as a compelling battery of SM tests.

183 3.2 EW measurements and SM tests at the LHeC

184 We note that, like the EIC, extensive DIS measurements at the LHeC would yield a large,
 185 $\int dt \mathcal{L} \sim 1 - 2 \text{ ab}^{-1}$, data set; the high-precision constraints from this information to nucleon-
 186 level PDFs and related quantities will therefore impose tight bounds on many PDF-dependent
 187 SM quantities, including Higgs and EW cross sections. Given its access to higher energies,
 188 however, the sizes of cross sections for many production processes in the Higgs and EW sectors
 189 will be sufficiently large as to allow precise measurements through DIS production for the first
 190 time. In fact, a variety of direct probes of EW and Higgs physics will therefore be available; as
 191 with the EIC-specific discussion in Sec. 2, we cannot review all of these, but instead highlight
 192 a small number of representative examples.

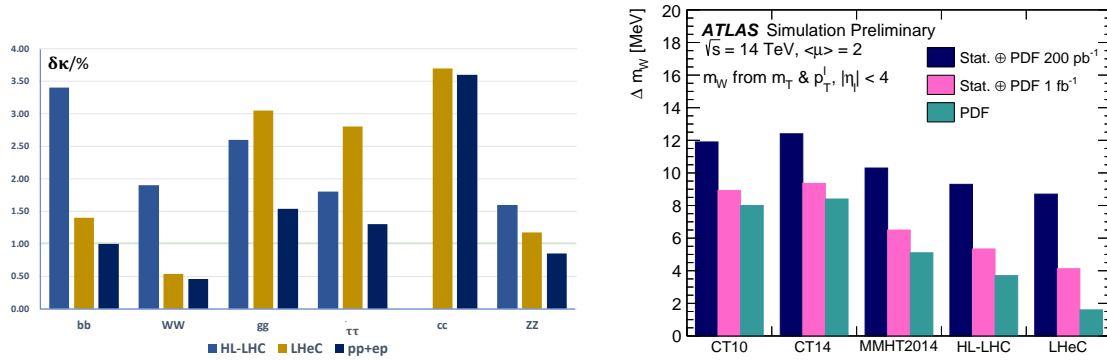


Figure 5: Through direct DIS production, the LHeC will have substantial constraining power over a variety of high-energy observables which will impact the HL-LHC program. Inclusion of LHeC pseudodata reduces the uncertainty in determinations of the BSM couplings of the Higgs boson (left) to the percent-level or less, particularly for the bb , WW , and ZZ channels. Similarly, PDF improvements driven by the LHeC can dramatically reduce the W -mass uncertainty, Δm_W (right), by greater than a factor of 2 relative to an HL-LHC-only scenario. Both panels are taken from the recent LHeC whitepaper, Ref. [5].

193 In the Higgs sector, the LHeC would substantially complement the reach of the HL-LHC,
 194 particularly given the predominance of alternate production channels in high-energy DIS like

195 $WW \rightarrow H$, in contrast to $gg \rightarrow H$, which is dominant in pp collisions. This complementarity
 196 can be illustrated quantitatively using the κ_i framework [17], wherein anomalous channel-
 197 specific deviations from the SM Higgs couplings are parametrized via effective couplings,
 198 κ_i . The result of a simultaneous analysis of 10 independent κ_i couplings was undertaken
 199 in Ref. [5], and we underscore the projected impact from separate HL-LHC and LHeC pseudo-
 200 data sets in the left panel of Fig. 5 for several Higgs decay channels of interest. In addition, the
 201 improvement in the uncertainties, $\delta\kappa_i$, achieved in a combined analysis of pp and ep data is
 202 also shown, highlighting the effect of fully leveraging the complementary hadroproduction and
 203 DIS data. The unique constraining power of the LHeC can be seen in the sharp improvements
 204 in the Higgs couplings to bb and WW , for which knowledge approaches the (sub)percent level
 205 only after including the high-precision LHeC data set.

206 The impact of highly constraining data at the LHeC will not be confined to the Higgs sector,
 207 but will also influence standard-candle EW observables, including extractions of m_W as shown
 208 in the right panel of Fig. 5. While the upgraded tracking detector at the HL-LHC will afford a
 209 greater coverage in the pseudorapidity of the W -boson decay lepton, $|\eta_l| < 4$, extractions of
 210 m_W from so-called template fits, in which m_W is tuned in simulations of the kinematic peaks of
 211 final-state distributions, remain PDF dependent. The resulting PDF uncertainty can be as large
 212 as $\Delta m_W = \pm 9$ MeV in contemporary determinations based on ATLAS data [18]. Extractions
 213 based, however, on future PDF sets [19] constrained by HL-LHC or LHeC data (the rightmost
 214 columns shown in Fig. 5), will have dramatically reduced PDF uncertainties, particularly in the
 215 case of LHeC inputs, for which the PDF uncertainty is projected to be as low as $\Delta m_W = \pm 1.6$
 216 MeV.

217 4 Conclusion

218 The coming decade promises a quickening pace in addressing many of the questions at the
 219 heart of QCD with the future precision DIS programs planned at the EIC and possible at the
 220 LHeC. We stress that these programs will leverage a strong mutual complementarity with ac-
 221 tivities at the HL-LHC as well as a number of ongoing or planned experiments from JLab12 to
 222 the neutrino DIS programs at DUNE [2], FASER ν [20], and elsewhere. Exploiting this comple-
 223 mentarity will require a continuation of the theoretical improvements necessary to describe
 224 hadronic data at a wide range of kinematical scales and the incorporation of the resulting
 225 knowledge into simulations, event-generator calculations, and ongoing detector design. De-
 226 velopment and coordination of these components remains ongoing within the Snowmass 2021
 227 exercises.

228 Acknowledgements

229 I would like to thank my CTEQ-TEA and nCTEQ colleagues for valuable inputs to this work,
 230 with special thanks to Alberto Accardi, Sayipjamal Dulat, T.-J. Hou, Xiaoxian Jing, Olek Kusina,
 231 Pavel Nadolsky, Fred Olness, Bo-Ting Wang, and C.-P. Yuan for providing helpful contributions
 232 and suggestions. I also acknowledge numerous valuable recommendations made by mem-
 233 bers of the EIC and LHeC communities, including Ludovica Aperio Bella, Abhay Deshpande,
 234 Claire Gwenlyn, Douglas Higinbotham, Max Klein, Ute Klein, and Rik Yoshida. This work was
 235 supported by the U.S. Department of Energy under Grant No. DE-SC0010129 as well as by
 236 a JLab EIC Center Fellowship. Additional support was provided by the Fermi National Ac-
 237 celerator Laboratory, managed and operated by Fermi Research Alliance, LLC under Contract
 238 No. DE-AC02-07CH11359 with the U.S. Department of Energy.

239 **References**

- 240 [1] G. Apollinari, I. Béjar Alonso, O. Bruning, P. Fessia, M. Lamont, L. Rossi and L. Tavian,
241 *High-Luminosity Large Hadron Collider (HL-LHC): Technical Design Report V. 0.1*, CERN
242 Technical Design Report V. 0.1 **4/2017** (2017), doi:[10.23731/CYRM-2017-004](https://doi.org/10.23731/CYRM-2017-004).
- 243 [2] R. Acciarri *et al.*, *Long-Baseline Neutrino Facility (LBNF) and Deep Underground Neutrino*
244 *Experiment (DUNE): Conceptual Design Report, Volume 2: The Physics Program for DUNE*
245 *at LBNF* (2015), [1512.06148](https://arxiv.org/abs/1512.06148).
- 246 [3] R. Abdul Khalek *et al.*, *Science Requirements and Detector Concepts for the Electron-Ion*
247 *Collider: EIC Yellow Report* (2021), [2103.05419](https://arxiv.org/abs/2103.05419).
- 248 [4] A. Accardi *et al.*, *Electron Ion Collider: The Next QCD Frontier*, Eur. Phys. J. **A52**(9), 268
249 (2016), doi:[10.1140/epja/i2016-16268-9](https://doi.org/10.1140/epja/i2016-16268-9), [1212.1701](https://arxiv.org/abs/1212.1701).
- 250 [5] P. Agostini *et al.*, *The Large Hadron-Electron Collider at the HL-LHC* (2020), [2007.14491](https://arxiv.org/abs/2007.14491).
- 251 [6] S. Alekhin *et al.*, *HERAFitter*, Eur. Phys. J. C **75**(7), 304 (2015),
252 doi:[10.1140/epjc/s10052-015-3480-z](https://doi.org/10.1140/epjc/s10052-015-3480-z), [1410.4412](https://arxiv.org/abs/1410.4412).
- 253 [7] T. J. Hobbs, J. T. Londergan, D. P. Murdock and A. W. Thomas, *Testing Partonic*
254 *Charge Symmetry at a High-Energy Electron Collider*, Phys. Lett. B **698**, 123 (2011),
255 doi:[10.1016/j.physletb.2011.02.040](https://doi.org/10.1016/j.physletb.2011.02.040), [1101.3923](https://arxiv.org/abs/1101.3923).
- 256 [8] B.-T. Wang, T. J. Hobbs, S. Doyle, J. Gao, T.-J. Hou, P. M. Nadolsky and F. I. Olness,
257 *Mapping the sensitivity of hadronic experiments to nucleon structure*, Phys. Rev. **D98**(9),
258 094030 (2018), doi:[10.1103/PhysRevD.98.094030](https://doi.org/10.1103/PhysRevD.98.094030), [1803.02777](https://arxiv.org/abs/1803.02777).
- 259 [9] J. Arrington *et al.*, *Revealing the structure of light pseudoscalar mesons at the electron-ion*
260 *collider*, J. Phys. G **48**(7), 075106 (2021), doi:[10.1088/1361-6471/abf5c3](https://doi.org/10.1088/1361-6471/abf5c3), [2102.11788](https://arxiv.org/abs/2102.11788).
- 261 [10] J. Dove *et al.*, *The asymmetry of antimatter in the proton*, Nature **590**(7847), 561 (2021),
262 doi:[10.1038/s41586-021-03282-z](https://doi.org/10.1038/s41586-021-03282-z), [2103.04024](https://arxiv.org/abs/2103.04024).
- 263 [11] M. Guzzi *et al.*, *NNLO constraints on proton PDFs from the SeaQuest and STAR experiments*
264 *and other developments in the CTEQ-TEA global analysis* (2021), [2108.06596](https://arxiv.org/abs/2108.06596).
- 265 [12] T.-J. Hou *et al.*, *New CTEQ global analysis of quantum chromodynamics with*
266 *high-precision data from the LHC*, Phys. Rev. D **103**(1), 014013 (2021),
267 doi:[10.1103/PhysRevD.103.014013](https://doi.org/10.1103/PhysRevD.103.014013), [1912.10053](https://arxiv.org/abs/1912.10053).
- 268 [13] A. Bacchetta, G. Bozzi, M. Radici, M. Ritzmann and A. Signori, *Effect of Flavor-Dependent*
269 *Partonic Transverse Momentum on the Determination of the W Boson Mass in Hadronic*
270 *Collisions*, Phys. Lett. B **788**, 542 (2019), doi:[10.1016/j.physletb.2018.11.002](https://doi.org/10.1016/j.physletb.2018.11.002), [1807.](https://arxiv.org/abs/1807.02101)
271 [02101](https://arxiv.org/abs/1807.02101).
- 272 [14] M. Arratia, Y. Furlotova, T. J. Hobbs, F. Olness and S. J. Sekula, *Charm jets as a probe*
273 *for strangeness at the future Electron-Ion Collider*, Phys. Rev. D **103**(7), 074023 (2021),
274 doi:[10.1103/PhysRevD.103.074023](https://doi.org/10.1103/PhysRevD.103.074023), [2006.12520](https://arxiv.org/abs/2006.12520).
- 275 [15] K. S. Kumar, A. Deshpande, J. Huang, S. Riordan and Y. X. Zhao, *Elec-*
276 *troweak and BSM Physics at the EIC*, EPJ Web Conf. **112**, 03004 (2016),
277 doi:[10.1051/epjconf/201611203004](https://doi.org/10.1051/epjconf/201611203004).

- 278 [16] R. Boughezal, F. Petriello and D. Wiegand, *Removing flat directions in standard model*
279 *EFT fits: How polarized electron-ion collider data can complement the LHC*, Phys. Rev. D
280 **101**(11), 116002 (2020), doi:[10.1103/PhysRevD.101.116002](https://doi.org/10.1103/PhysRevD.101.116002), [2004.00748](https://arxiv.org/abs/2004.00748).
- 281 [17] J. de Blas *et al.*, *Higgs Boson Studies at Future Particle Colliders*, JHEP **01**, 139 (2020),
282 doi:[10.1007/JHEP01\(2020\)139](https://doi.org/10.1007/JHEP01(2020)139), [1905.03764](https://arxiv.org/abs/1905.03764).
- 283 [18] M. Aaboud *et al.*, *Measurement of the W-boson mass in pp collisions at $\sqrt{s} = 7$ TeV with*
284 *the ATLAS detector*, Eur. Phys. J. C **78**(2), 110 (2018), doi:[10.1140/epjc/s10052-017-](https://doi.org/10.1140/epjc/s10052-017-5475-4)
285 [5475-4](https://doi.org/10.1140/epjc/s10052-017-5475-4), [Erratum: Eur.Phys.J.C 78, 898 (2018)], [1701.07240](https://arxiv.org/abs/1701.07240).
- 286 [19] *Prospects for the measurement of the W-boson mass at the HL- and HE-LHC*, Tech.
287 rep., CERN, Geneva, All figures including auxiliary figures are available at
288 [https://atlas.web.cern.ch/Atlas/GROUPS/PHYSICS/PUBNOTES/ATL-PHYS-PUB-](https://atlas.web.cern.ch/Atlas/GROUPS/PHYSICS/PUBNOTES/ATL-PHYS-PUB-2018-026)
289 [2018-026](https://atlas.web.cern.ch/Atlas/GROUPS/PHYSICS/PUBNOTES/ATL-PHYS-PUB-2018-026) (2018).
- 290 [20] H. Abreu *et al.*, *Technical Proposal: FASERnu* (2020), [2001.03073](https://arxiv.org/abs/2001.03073).